Journal of Non-Crystalline Solids 355 (2009) 1307–1312

Contents lists available at ScienceDirect

Journal of Non-Crystalline Solids

journal homepage: www.elsevier.com/locate/jnoncrysol

On the effect of hydrostatic pressure on the auxetic character of NAT-type silicates

Joseph N. Grima *, Richard N. Cassar, Ruben Gatt

Department of Chemistry, University of Malta, Msida MSD 2080, Malta

ARTICLE INFO

Article history:
Available online 22 June 2009

PACS:
62.20.-x
62.20.dj
62.20.de
62.20.dq

Keywords:
Mechanical properties
Auxetic
Pressure
NAT
Natrolite
Negative poisson's ratio
Zeolites

ABSTRACT

Materials with negative Poisson's ratios (auxetics) exhibit the property of expanding laterally when uniaxially stretched and becoming narrower when compressed. A system which exhibits this unexpected property is natrolite (NAT), a zeolite which is auxetic in its (0 0 1) plane. Here, we examine the effect of external hydrostatic pressure on the crystal structure of hypothetical silicates equivalent to frameworks in the NAT group. We show that the crystal structure and mechanical properties of the SiO_2 equivalents of the NAT, THO (thomsonite) and EDI (edingtonite) frameworks are highly pressure dependent and that these systems are most auxetic at non-ambient conditions, in particular at positive external hydrostatic pressures which are predicted to be approximately 2–8% of the bulk modulus. An attempt is made to explain this pressure dependency of the Poisson's ratio in terms of the framework geometry and the deformation mechanism.

1. Introduction

Materials with a negative Poisson's ratio (NPR) exhibit the unusual property of expanding when stretched and getting thinner when compressed [1–5]. Such materials, also known as auxetics [1], are not commonly encountered in everyday applications, however due to the increased interest in their properties, there has been an effort at identifying naturally occurring auxetics and to design new man-made auxetics [2–48]. Such materials range from microstructured materials (e.g. foams [10–15] and microporous polymers [16–18]) to molecular-level auxetics such as polymers [1,19–23], metals [24], silicates [25–33,38] and zeolites [34,36,44–47,49]. These materials are characterized by some particular geometry (at the nano-, micro-, or macro-structural level) that allows auxetic behavior through specific deformation mechanisms, and in recent years, a number of studies [10–15,34,36,40–45,48,49] have proposed various two or three dimensional models which can explain the occurrence of negative Poisson's ratios.

A class of auxetic materials that has gathered much interest in recent years is that of zeolites [34–36,44–47,49]. Evidence of auxeticity in the zeolite class of materials was first reported in 1999 [35], where it was reported that simulations had predicted that various zeolites including members of the natrolite group (in particular NAT, EDI and THO) may exhibit this anomalous property in particular crystallographic planes. These predictions were backed up by further theoretical and experimental work where, for example, experimental work using a Brillouin light scattering technique, determined that NAT crystals exhibit NPR which is at a maximum in the (0 0 1) plane for loading at approximately 45° off-axis [46,47]. Furthermore, modeling studies on NAT-type systems showed that their negative Poisson's ratio in the (0 0 1)-plane may be explained in terms of a 2D model based on semi-rigid rotating squares/parallelograms [34,35,41,42,44,49–51].

Although it is well known that pressure and/or temperature can affect the magnitude of the Poisson's ratio [7,9,31,52–56], no work has as yet been performed to assess the effect of external hydrostatic pressure on the elastic constants of zeolite-type frameworks, in particular, the way that external pressure can affect the Poisson's ratio. In view of this, here we will report preliminary work on the SiO_2 equivalent of the zeolites NAT, THO and EDI in an attempt to assess how hypothetical frameworks in the natrolite group respond to changes in the external hydrostatic pressure and also how such changes effect the extent of auxeticity.

2. Method

Simulations were performed on the all silica equivalent of the empty NAT framework (i.e. a system which is equivalent to NAT

* Corresponding author.
E-mail address: joseph.grima@um.edu.mt (J.N. Grima).

0022-3093/$ - see front matter © 2009 Elsevier B.V. All rights reserved.
doi:10.1016/j.jnoncrysol.2009.05.018

without any cations or water molecules and with all the aluminum atoms in the framework substituted by silicon atoms), henceforth referred to as NAT–Si using the Cerius^2 molecular modeling package running on an SGI Octane 2 workstation. The NAT–Si framework was aligned in space in such a way that the [0 0 1] direction of the crystal was fixed parallel to the *Z*-direction whilst the [0 1 0] direction was fixed to lie in the *YZ* plane. Energy expressions were set using the COMPASS and the CVFF 300 force-fields as implemented in Cerius^2 V4.1 (Accelrys Inc.), two force-fields which are fully parameterised for modeling of silicate frameworks [57] and have been shown to be the best force-fields for reproducing the experimentally measured Poisson's ratio in the silicate α-cristobalite [58]. These force-fields contain bond terms (stretching terms, angle bending terms and torsion terms), cross-terms, and non-bond terms (van der Waal and electrostatic terms), where in the case of the CVFF force-field the stretching terms are described by a Morse term, the angle bending terms are described by harmonic term, the torsion term by an scaled dihedral term and van der Waal term is a Lennard Jones 12-6 whist in the case of the COMPASS force-field the stretching and angle bending terms are described by quartic terms, the torsion terms are described by dihedral terms whilst the van der Waal term is a Lennard Jones 9-6.

All non-bond terms were summed up using the Ewald summation technique [59] whilst all other settings and parameters where as defined in the respective force-fields as implemented in Cerius^2 Version 4.1. For both force-fields, a series of energy minimisations using the SMART compound minimiser were carried out to the default Cerius^2 high convergence criteria whilst the system was subjected to both positive and negative external hydrostatic pressures *P*, i.e. whilst the system was subjected to stresses defined by:

$$\sigma_{ij} = -\begin{pmatrix} P & 0 & 0 \\ 0 & P & 0 \\ 0 & 0 & P \end{pmatrix}$$

The mechanical properties, in particular the on-axis stiffness and compliance matrices, the on-axis Young's moduli and the on-axis Poisson's ratio for each of these minimized systems were then calculated using the second derivative method in accordance with the procedure followed by Alderson et al. [31]. The off-axis Young's moduli and the on-axis Poisson's ratios in the (0 0 1) plane were also calculated using standard axis-transformation techniques [60]. Similar simulations were carried out for the SiO_2 equivalents of the THO and EDI frameworks (henceforth referred to as THO–Si and EDI–Si).

An attempt was also made to identify the underlying cause for the particular values of the predicted Poisson's ratios by simulating the atomic level deformations of the NAT–Si systems at various stresses σ at 45° to the *X* and *Y* axis (a direction of maximum auxeticity) whilst still being subjected to a hydrostatic pressure *P* by performing energy minimisations whilst the system is being subjected to the following loading conditions:

$$\sigma_{ij} = -\begin{pmatrix} P & 0 & 0 \\ 0 & P & 0 \\ 0 & 0 & P \end{pmatrix} + \frac{1}{2}\begin{pmatrix} \sigma & -\sigma & 0 \\ -\sigma & \sigma & 0 \\ 0 & 0 & 0 \end{pmatrix}.$$

3. Results and discussion

The cell parameters, mechanical properties and various geometrical features related to the (0 0 1) projections for the various simulated NAT–Si systems are displayed graphically in Fig. 1 (cell parameters), Fig. 2 (Young's moduli and bulk moduli), Fig. 3 (Poisson's ratio) and Fig. 4 (geometric parameters related to the (0 0 1)

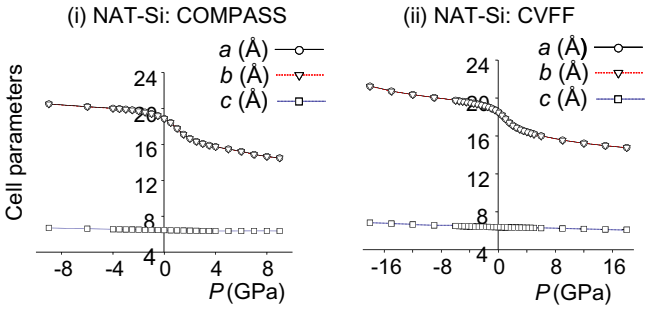

Fig. 1. The cell parameters for NAT–Si under various pressures as simulated by the different force-fields. Note that the cell angles *a*, *b* and *c* were found to remain approximately constant at 90°.

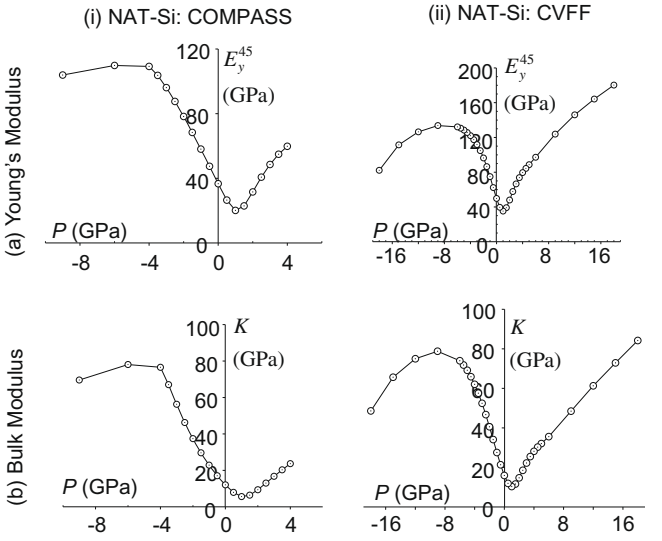

Fig. 2. The Young's moduli in the [1 1 0] direction and bulk moduli for NATSi under various pressures as simulated by the different force-fields.

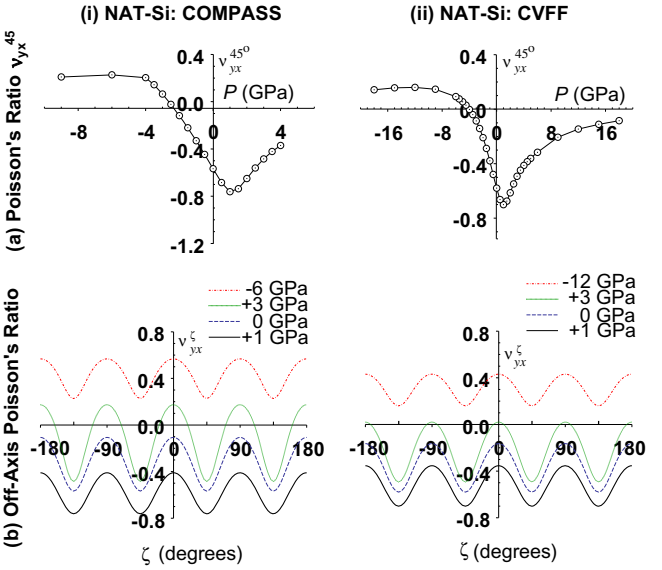

Fig. 3. (i) The Poisson's ratio in the (0 0 1) plane for loading in the [1 1 0] direction for NAT–Si under various pressures as simulated by the different force-fields. (ii) Profiles of the off-axis Poisson's ratios v^{ζ}_{xy} in the (0 0 1) plane at four different pressures.

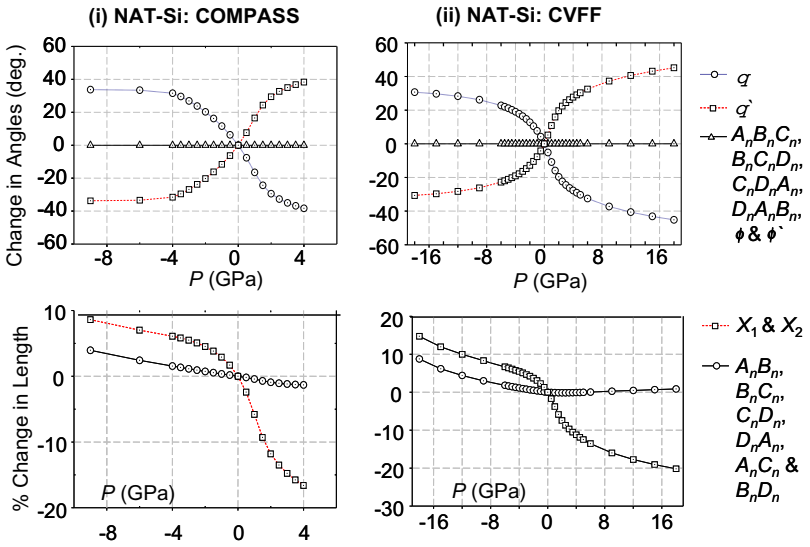

Fig. 4. The variation of various (i) dimensions and (ii) angles projected in the (0 0 1) plane for NAT–Si as a result of pressure changes as simulated by the different force-fields. Note that the variations in the lengths are shown as percentage changes compared to the respective systems at $P = 0$ GPa whilst the variations in the angles are shown as absolute changes in degrees compared to the respective systems at $P = 0$ GPa.

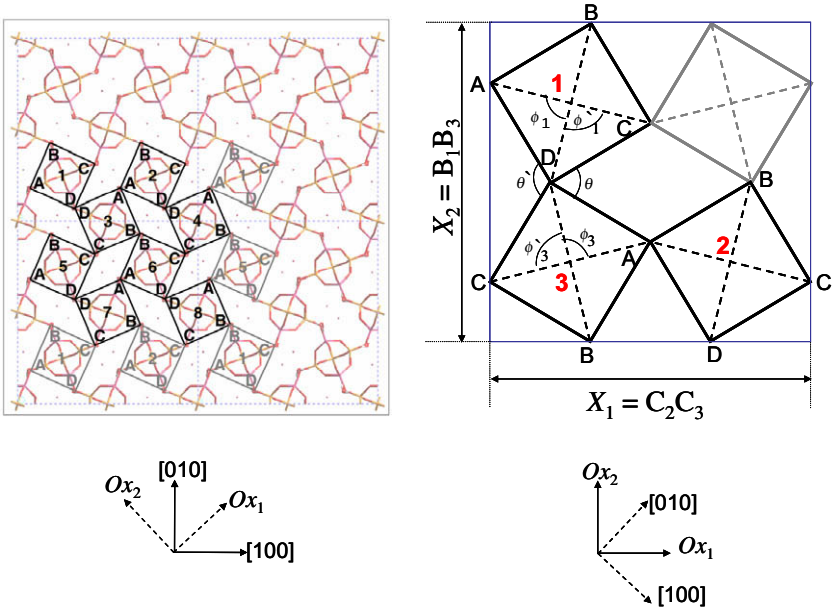

Fig. 5. The parameters measured and plotted in Figs. 4 and 7.

plane, see Fig. 5 for definition of parameters measured). The data related to THO–Si and EDI–Si obtained using the Burchart force-field are displayed graphically in Figs. 6 and 7 respectively. Also shown in Fig. 8 are some images of the projection of the NAT–Si systems in the (0 0 1) plane at various pressures.

These results clearly suggest that for all systems, irrespective of the force-field and/or system used, the applied pressure results in a significant change in the a and b dimensions of the unit cell with a much lower change in c. This was to be expected given that the Young's moduli E_x and E_y are significantly lower than E_z and is due to the fact that these systems may easily deform through the 'rotating squares' mechanism in the (0 0 1) plane (the XY plane) [34,35,44,49–51]. The fact that the 'rotating squares' mechanism is indeed operating when the systems are placed under hydrostatic pressure is supported not only by the images in Fig. 8 but also from measurements of various projected dimensions and angles. In fact, irrespective of the force-field and/or system used, when various geometrical parameters related to the projected 'rotating squares' in the (0 0 1) plane were measured, it was found that the application of pressure resulted in significant changes in the angles between the projected squares when compared to the lengths of the sides and of the diagonals of the projected squares, the internal angles of the squares and the angles between the diagonals of the projected squares (see Figs. 4 and 5 for data related to NAT–Si). It is interesting to note that at the higher values of negative hydrostatic pressures, the projected squares are in their 'fully open conformation' (see Fig. 8).

We also found that irrespective of the force-field and/or system used, the Poisson's ratios in the (0 0 1) plane are dependent on the applied hydrostatic pressure. We found that maximum auxeticity

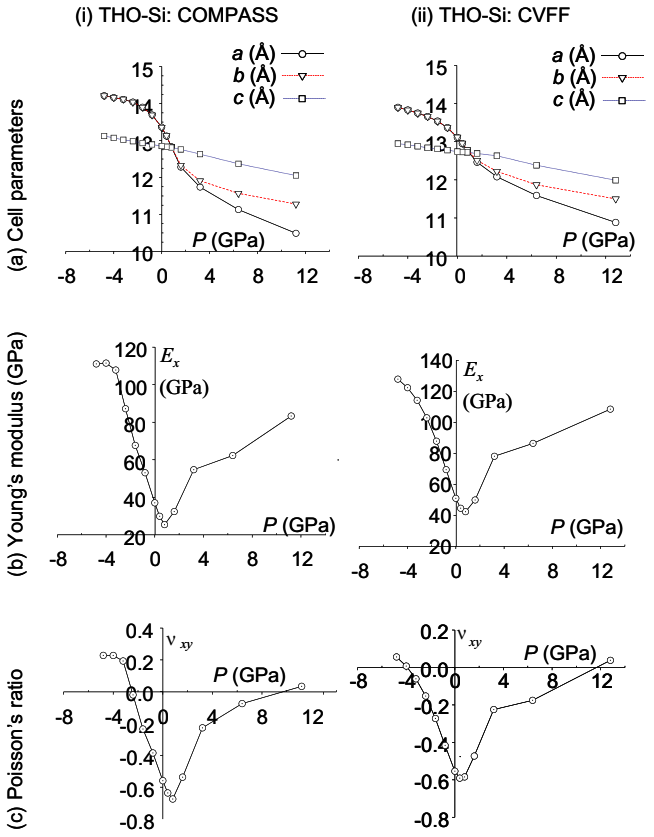

Fig. 6. The data related to THO as simulated by the COMPASS and CVFF force-fields.

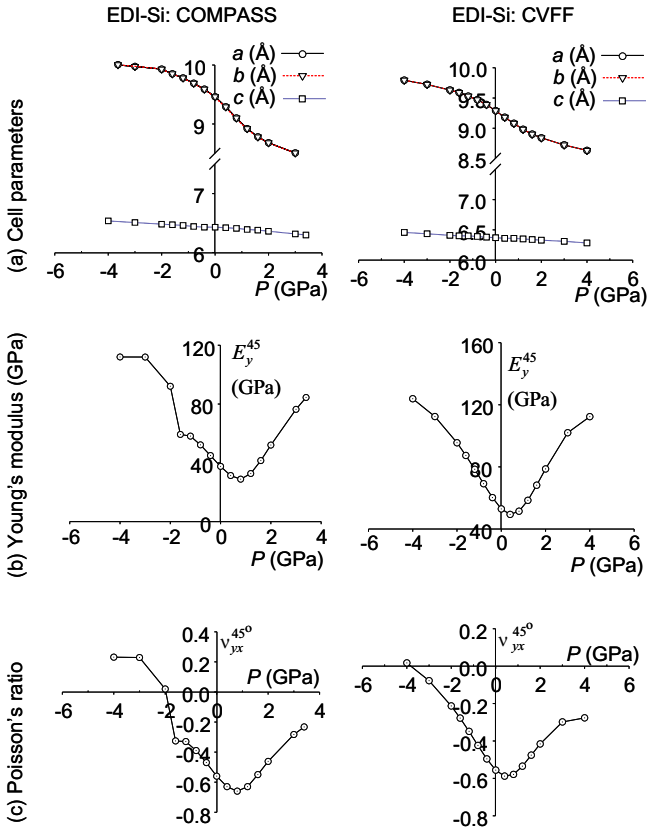

Fig. 7. The data related to EDI as simulated by the COMPASS and CVFF force-fields.

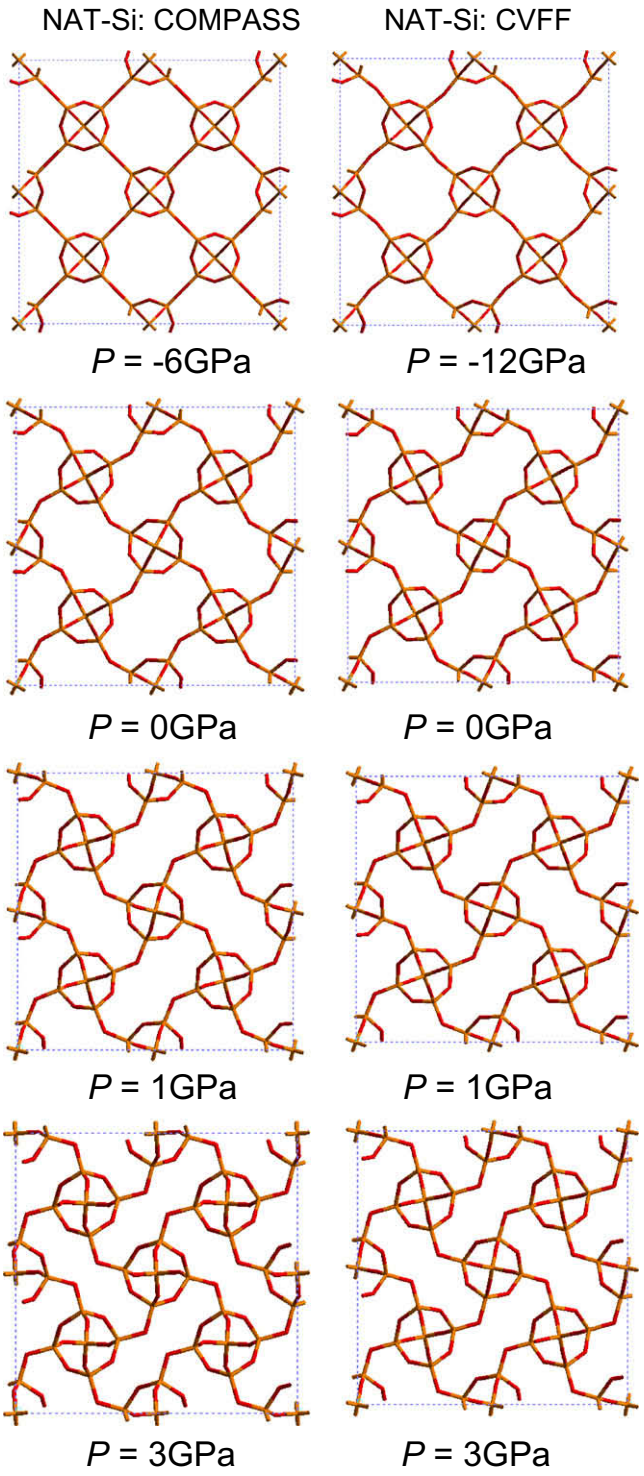

Fig. 8. Images of NAT–Si in the (0 0 1) plane at various pressures as simulated by the COMPASS and CVFF force-fields.

is not exhibited at zero applied pressure (i.e. at atmospheric pressure) but at a positive hydrostatic pressure, which in the case of NAT–Si was predicted to be 1.0 GPa by the COMPASS force-field and the CVFF force-field, i.e. at pressures which are around 6–8% of the predicted bulk modulus[1] by the respective force-field at zero

[1] Note that the bulk modulus was also found to be pressure dependent as illustrated in Fig. 2.

pressure (8% of K in the case of the COMPASS force-field and 6% of K in the case of the CVFF force-field where K is the bulk modulus at zero pressure[1], predicted to be 12.0 GPa by the COMPASS force-field and 15.9 GPa by the CVFF force-field). In this respect we note that our results appear to provide an exceptional case to the hypothesis proposed by Wojciechowski et al. [56] which suggests in general, negative hydrostatic pressure can transform conventional materials into auxetics. Our exception to Wojciechowski's hypothesis is likely to be due to the very particular nanostructure of NAT and the way it deforms when subjected to mechanical loads may be explained below.

We found that as the pressure deviates from this optimum pressure for auxeticity, the auxetic nature of NAT–Si decreases, a phenomenon that is normally more pronounced under negative pressures (i.e. as the angles between the projected squares increase) than under positive pressures (i.e. as the angles between the projected squares decrease).

Similar properties were predicted by these force-fields for THO–Si and EDI–Si where maximum auxeticity was predicted to occur at approximately 2–7% of the bulk modulus at zero pressure.

When we analyzed the minimized systems which were subjected to a combined hydrostatic pressure and uniaxial stress (see Table 1), we found that the most auxetic systems were characterized with a deformation profile where the 'rotating squares' mechanism operates most effectively in the sense that the angles between the squares change to the greatest extent when compared to the other geometrical parameters measured. In all of the other systems we observed that as the auxeticity becomes less pronounced, the squares themselves start to deform to a greater extent when compared to the extent of rotation of the squares. In fact, in the most extreme cases when the squares were fully open relative to each other, we observed that although there were changes in the angles between the squares, these changes in angles where accompanied by comparable changes in the internal angles of the squares with the net result that there is little or no net relative rotations of the squares.

This variation of the Poisson's ratio with hydrostatic pressure can be explained in terms of deviations from the idealized 'rotating rigid squares' model which predicts Poisson's ratios of $v_{ij}^{\text{rot-sqr}} = -1$.

In reality, an idealized scenario where projected squares behave as perfectly rigid bodies is difficult to accomplish and in fact, our simulations predict that even in the most auxetic systems, rotation of the squares is always accompanied by other deformation mechanisms which result in deformations of the squares themselves.

If we assume that in the real scenario the 'rotating rigid squares' are replaced by 'rotating semi-rigid squares' and that these additional modes of deformations that accompany the idealized 'rotating rigid squares' mechanism have Poisson's ratio and Young's moduli given by v_{ij}^{other} and E_i^{other}, then for loading by a stress σ_i in an Ox_i direction, the total strains in the Ox_i direction are given by $\varepsilon_i^{\text{total}} = \varepsilon_i^{\text{rot-sqr}} + \varepsilon_i^{\text{other}}$.

Since a strain ε_i in an Ox_i direction and a strain in the orthogonal Ox_j direction are related to a stress σ_i in the Ox_i direction through:

$$\varepsilon_i = \frac{1}{E_i}\sigma_i \quad \varepsilon_j = -v_{ij}\varepsilon_i = \frac{-v_{ij}}{E_i}\sigma_i, \tag{1}$$

where E_i is the Young's modulus in the Ox_i direction and v_{ij} is the Poisson's ration in the Ox_i–Ox_j plane for loading in the Ox_i direction, then we note that E_i^{total} and v_{ij}^{total}, the overall Young's modulus in the Ox_i direction and the overall Poisson's ration in the Ox_i–Ox_j plane for loading in the Ox_i direction due to the 'rotating squares' mechanism and other concurrent mechanisms, may be defined through:

$$\frac{1}{E_i^{\text{total}}} = \frac{1}{E_i^{\text{rot-sqr}}} + \frac{1}{E_i^{\text{other}}}, \quad \frac{v_{ij}^{\text{total}}}{E_i^{\text{total}}} = \frac{v_{ij}^{\text{rot-sqr}}}{E_i^{\text{rot-sqr}}} + \frac{v_{ij}^{\text{other}}}{E_i^{\text{other}}}. \tag{2}$$

All this clearly suggests that the contribution to the overall Poisson's ratio of the '−1 Poisson's ratio' which arises from the idealized 'rotating squares' mechanism decreases as the Young's moduli associated with the idealized 'rotating squares' mechanism increase. Thus, since the analytical model derived for the idealized model predicts Young's moduli of:

$$E_i^{\text{rot-sqr}} = K_h \frac{8}{zl^2} \frac{1}{[1-\sin(\theta)]}.$$

where K_h is the hinging constant, l is the length of the sides of the squares, θ is the angle between the squares and z is the thickness in the third direction, then as $\theta \to 90^\circ$, i.e. as the squares approach their most open conformation, the total Poisson's ratio is not expected to remain dominated by the auxetic contribution since the Young's moduli of the idealized 'rotating squares' structure increases to the extent that, when $\theta = 90^\circ$, the Young's moduli for the idealized 'rotating squares' mode of deformation would have been infinite (structure is locked) and thus the observed Poisson's ratio and Young's moduli would become equal to v_{ij}^{other} and E_i^{other} respectively (i.e. the rotating squares mechanism plays no role), thus explaining the behavior of the systems at higher negative pressures.

Table 1
The variation of various (i) dimensions and (ii) angles projected in the (0 0 1) plane for loading in the [1 1 0] direction for NAT–Si under various pressures as simulated by the different force-fields. The parameters are defined in Fig. 5. Note that the variations in the lengths are shown as percentage changes compared to the respective systems at $\sigma = 0$ GPa whilst the variations in the angles are shown as absolute changes in degrees compared to the respective systems at $\sigma = 0$ GPa.

		% Change in lengths								Changes in angles (°)						
	P (GPa)	A_1B_1	B_1C_1	C_1D_1	D_1A_1	A_1C_1	B_1D_1	X_1	X_2	$A_1B_1C_1$	$B_1C_1D_1$	$C_1D_1A_1$	$D_1A_1B_1$	φ_1	θ	θ'
COMPASS	−6.00	0.34	0.35	0.34	0.35	−0.18	0.87	−0.18	0.87	−0.60	0.60	−0.60	0.60	0.00	0.69	0.51
	−3.00	0.23	0.44	0.23	0.44	−0.19	0.87	−0.05	1.02	−0.61	0.61	−0.61	0.61	0.12	3.48	−2.26
	−1.00	0.08	0.56	0.08	0.56	−0.20	0.84	0.59	1.73	−0.60	0.60	−0.60	0.60	0.28	5.51	−4.32
	0.00	0.03	0.59	0.03	0.59	−0.19	0.82	1.55	2.73	−0.58	0.58	−0.58	0.58	0.32	7.49	−6.33
	1.00	0.08	0.72	0.08	0.72	−0.04	0.84	3.44	4.64	−0.51	0.51	−0.51	0.51	0.37	9.41	−8.39
	2.00	−0.07	0.59	−0.07	0.59	−0.10	0.62	1.84	2.97	−0.41	0.41	−0.41	0.41	0.38	4.42	−3.59
	3.00	−0.16	0.48	−0.16	0.48	−0.17	0.48	0.90	1.99	−0.37	0.37	−0.37	0.37	0.37	2.53	−1.77
CVFF	−12.00	0.28	0.35	0.28	0.35	−0.10	0.72	−0.08	0.75	−0.47	0.47	−0.47	0.47	0.04	0.74	0.20
	−6.00	0.17	0.35	0.17	0.35	−0.12	0.64	−0.05	0.74	−0.44	0.44	−0.44	0.44	0.11	1.15	−0.27
	−3.00	0.10	0.37	0.10	0.37	−0.14	0.61	0.09	0.89	−0.43	0.43	−0.43	0.43	0.16	1.96	−1.10
	0.00	−0.05	0.39	−0.05	0.39	−0.18	0.52	1.16	2.01	−0.40	0.40	−0.40	0.40	0.25	5.13	−4.33
	1.00	−0.13	0.37	−0.13	0.37	−0.19	0.43	1.89	2.74	−0.36	0.36	−0.36	0.36	0.29	5.92	−5.20
	2.00	−0.17	0.35	−0.17	0.35	−0.19	0.36	1.19	2.00	−0.32	0.32	−0.32	0.32	0.30	3.46	−2.84
	3.00	−0.17	0.30	−0.17	0.30	−0.19	0.31	0.68	1.46	−0.29	0.29	−0.29	0.29	0.27	2.19	−1.62

The gradients of plots of % changes (for lengths) and actual changes (for angles in degrees) *vs.* applied stress at 45° to the *y*-direction (in GPa) for NAT–Si. These values represent the change (percentage or actual) in the various lengths of sides/diagonals of squares, etc. per 1 GPa applied stress.

The behavior of the systems under high positive pressures which are predicted to exhibit a lower extent of auxeticity may be explained by the fact that our molecular systems are much more complex than simple mechanical systems as our silicates are in reality composed of atoms which interact with each other, which interactions become much more pronounced as the separation between the atoms decreases, something which occurs at higher positive pressures. Such increased interactions restrict the idealized 'rotating squares' mechanism with the net result that the auxetic character decreases at high positive pressures despite the fact that from a purely mechanistic point of view one would have expected an increase in the auxetic character. In fact, we argue that it is as a net result of all this that we observe the most negative Poisson's ratio at a low external positive hydrostatic pressure, as such conditions represent optimal conditions for auxeticity (i.e. the best balance between the 'pro-auxetic' nature that is a result of the proposed mechanism, and 'against-auxetic' nature due to atomic level effects).

Before we conclude this discussion, it is important to highlight that the work presented in this paper describes the behavior of the idealized SiO_2 equivalents of the empty zeolite frameworks, which behavior may not necessarily be mirrored in the real zeolite. In particular we note that whilst we expect that in such real systems the Poisson's ratio will also be highly dependent on the external hydrostatic pressure, maximum auxeticity may not necessarily occur at approximately 2–8% of the bulk moduli as the cations and water molecules present additional hindrance to the 'rotating squares' mechanism thus making the repulsive interactions which restrict the auxeticity at high positive pressures to become more pronounced.

4. Conclusion

This paper has shown that the external hydrostatic pressure has a significant effect on the crystal structure and mechanical properties of the SiO_2 equivalent of NAT-type systems. In particular we have shown that auxeticity is at a maximum at a positive hydrostatic pressure which is predicted to be within 2–8% of the bulk moduli at zero pressure. We argue that the decrease in the Poisson's ratio as the external hydrostatic pressure is increased can be explained in terms of the nanostructure of NAT-type frameworks and the way it deforms when subjected to mechanical loads. In particular, we show that increased auxeticity may be explained in terms of the projected 'rotating semi-rigid squares' model projected in the (0 0 1) plane, which effect becomes hindered as the separation between the squares becomes smaller due to interatomic repulsive interactions that are observed at short interatomic separations (hence the observed decrease in auxeticity at high positive pressures).

All this is very significant as it highlights the fact that the lowest values of the Poisson's ratio a system can exhibit may occur at non-ambient conditions. This suggests that if one has to analyze the whole pressure–temperature domain, one is likely to find auxeticity in systems which are conventional at ambient conditions.

Acknowledgements

The financial support of the Malta Council for Science and Technology through their national RTDI programme is gratefully acknowledged. We also acknowledge the contribution of Ms Daphne Attard of the University of Malta.

References

[1] K.E. Evans, M.A. Nkansah, I.J. Hutchinson, S.C. Rogers, Nature 353 (1991) 124.
[2] K.W. Wojciechowski, A. Alderson, K.L. Alderson, B. Maruszewski, F. Scarpa, Phys. Stat. Sol. B 244 (2007) 813.
[3] L.J. Gibson, M.F. Ashby, G.S. Schajer, C.I. Robertson, Proc. R. Soc. Lond. A 382 (1982) 25.
[4] R.F. Almgren, J. Elast. 15 (1985) 427.
[5] D. Prall, R.S. Lakes, Int. J. Mech. Sci. 39 (1997) 305.
[6] A. Spadoni, M. Ruzzene, F. Scarpa, Phys. Stat. Sol. B 242 (2005) 695.
[7] K.W. Wojciechowski, Mol. Phys. 61 (1987) 1247.
[8] K.W. Wojciechowski, A.C. Branka, Phys. Rev. A 40 (1989) 7222.
[9] K.W. Wojciechowski, J. Phys. A Math. Gen. 36 (2003) 11765.
[10] R.S. Lakes, Science 235 (1987) 1038.
[11] K.E. Evans, M.A. Nkansah, I.J. Hutchinson, Acta Metall. Mater. 2 (1994) 1289.
[12] J.B. Choi, R.S. Lakes, J. Compos. Mater. 29 (1995) 113.
[13] N. Chan, K.E. Evans, J. Cell. Plast. 34 (1998) 231.
[14] C.W. Smith, J.N. Grima, K.E. Evans, Acta Mater. 48 (2000) 4349.
[15] J.N. Grima, A. Alderson, K.E. Evans, J. Phys. Soc. Jpn. 74 (2005) 1341.
[16] K.E. Evans, B.D. Caddock, J. Phys. D Appl. Phys. 22 (1989) 1883.
[17] A. Alderson, K.E. Evans, J. Mater. Sci. 30 (1995) 3319.
[18] A. Alderson, K.E. Evans, J. Mater. Sci. 32 (1997) 2797.
[19] R.H. Baughman, D.S. Galvao, Nature 365 (1993) 635.
[20] C.B. He, P.W. Liu, A.C. Griffin, Macromolecules 31 (1998) 3145.
[21] J.N. Grima, K.E. Evans, Chem. Commun. (2000) 1531.
[22] J.N. Grima, J.J. Williams, K.E. Evans, Chem. Commun. (2005) 4065.
[23] G.Y. Wei, Phys. Stat. Sol. B 242 (2005) 742.
[24] R.H. Baughman, J.M. Shacklette, A.A. Zakhidov, S. Stafstrom, Nature 392 (1998) 362.
[25] A. Yeganeh-Haeri, D.J. Weidner, D.J. Parise, Science 257 (1992) 650.
[26] N.R. Keskar, J.R. Chelikowsky, Phys. Rev. B 46 (1992) 1.
[27] H. Kimizuka, H. Kaburaki, Y. Kogure, Phys. Rev. Lett. 84 (2000) 5548.
[28] A. Alderson, K.E. Evans, Phys. Rev. Lett. 89 (2002) 225503.
[29] H. Kimizuka, H. Kaburaki, Y. Kogure, Phys. Rev. B 67 (2003) 024105.
[30] A. Alderson, K.L. Alderson, K.E. Evans, J.N. Grima, M. Williams, J. Met. Nano Mater. 23 (2004) 55.
[31] A. Alderson, K.L. Alderson, K.E. Evans, J.N. Grima, M. Williams, P.J. Davies, Phys. Stat. Sol. B 242 (2005) 499.
[32] J.N. Grima, R. Gatt, A. Alderson, K.E. Evans, J. Mater. Chem. 15 (2005) 4003.
[33] J.N. Grima, R. Gatt, A. Alderson, K.E. Evans, Mater. Sci. Eng. A 423 (2006) 219.
[34] J.N. Grima, R. Jackson, A. Alderson, K.E. Evans, Adv. Mater. 12 (2000) 1912.
[35] J.N. Grima, A. Alderson, K.E. Evans, Zeolites with negative Poisson's ratios, in: Paper Presented at the RSC Fourth International Materials Conference (MC4), Dublin, Ireland, P81, July 1999.
[36] J.N. Grima, Ph.D. Thesis, University of Exeter, Exeter, UK, 2000.
[37] K.W. Wojciechowski, J. Phys. Soc. Jpn. 72 (2003) 1819.
[38] H. Kimizuka, S. Ogata, Y. Shibutani, Phys. Stat. Sol. B 244 (2007) 900.
[39] K.V. Tretiakov, K. Wojciechowski, Phys. Stat. Sol. B 244 (2007) 1038.
[40] J.N. Grima, K.E. Evans, J. Mater. Sci. 4 (2006) 3193.
[41] J.N. Grima, K.E. Evans, J. Mater. Sci. Lett. 19 (2000) 1563.
[42] Y. Ishibashi, M.J. Iwata, J. Phys. Soc. Jpn. 69 (2000) 2702.
[43] A. Alderson, K.L. Alderson, K.E. Evans, J.N. Grima, M.R. Williams, P.J. Davies, Comput. Meth. Sci. Technol. 10 (2004) 117.
[44] J.N. Grima, A. Alderson, K.E. Evans, Phys. Stat. Sol. B 242 (2005) 561.
[45] J.N. Grima, V. Zammit, R. Gatt, A. Alderson, K.E. Evans, Phys. Stat. Sol. B 244 (2007) 866.
[46] C. Sanchez-Valle, S.V. Sinogeikin, Z.A.D. Lethbridge, R.I. Walton, C.W. Smith, K.E. Evans, J.D. Bass, J. Appl. Phys. 98 (2005) 053508.
[47] J.N. Grima, R. Gatt, V. Zammit, J.J. Williams, K.E. Evans, A. Alderson, R.I. Walton, J. Appl. Phys. 101 (2007) 086102.
[48] J.N. Grima, R. Gatt, A. Alderson, K.E. Evans, J. Phys. Soc. Jpn. 74 (2005) 2866.
[49] J.J. Williams, C.W. Smith, K.E. Evans, Z.A.D. Lethbridge, R.I. Walton, Chem. Mater. 19 (2007) 2423.
[50] R. Gatt, V. Zammit, C. Caruana, J.N. Grima, Phys. Stat. Sol. B 245 (2008) 502.
[51] J.N. Grima, V. Zammit, R. Gatt, D. Attard, C. Caruana, T.G. Chircop Bray, J. Non. Cryst. Solids 354 (2008) 4304.
[52] D. Attard, J.N. Grima, Phys. Stat. Sol. B 245 (2008) 2395.
[53] K.W. Wojciechowski, Phys. Lett. A 137 (1989) 60.
[54] K.W. Wojciechowski, K.V. Tretiakov, M. Kowalik, Phys. Rev. E 67 (2003) 036121.
[55] K.W. Wojciechowski, in: B. Idzikowski, P. Svec, M. Miglierini (Eds.), Properties and Applications of Nanocrystalline Alloys from Amorphous Precursors, NATO Science Series II: Mathematics, Physics and Chemistry, vol. 184, Kluwer, 2005, p. 241.
[56] (a) K.W. Wojciechowski, Molec. Phys. Rep. 10 (1995) 129;
(b) K.W. Wojciechowski, K.V. Tretiakov, Comput. Meth. Sci. Technol. 1 (1995) 25.
[57] Cerius^2 User Manuals (and references cited within), Accelrys Inc., San Diego, USA.
[58] J.N. Grima, R. Gatt, V. Zammit, A. Alderson, K.E. Evans, Xjenza 10 (2005) 24.
[59] P.P. Ewald, Ann. Phys. (Leipzig) 64 (1921) 253.
[60] F. Nye, Physical Properties of Crystals, Clarendon, Oxford, 1957.